Figures

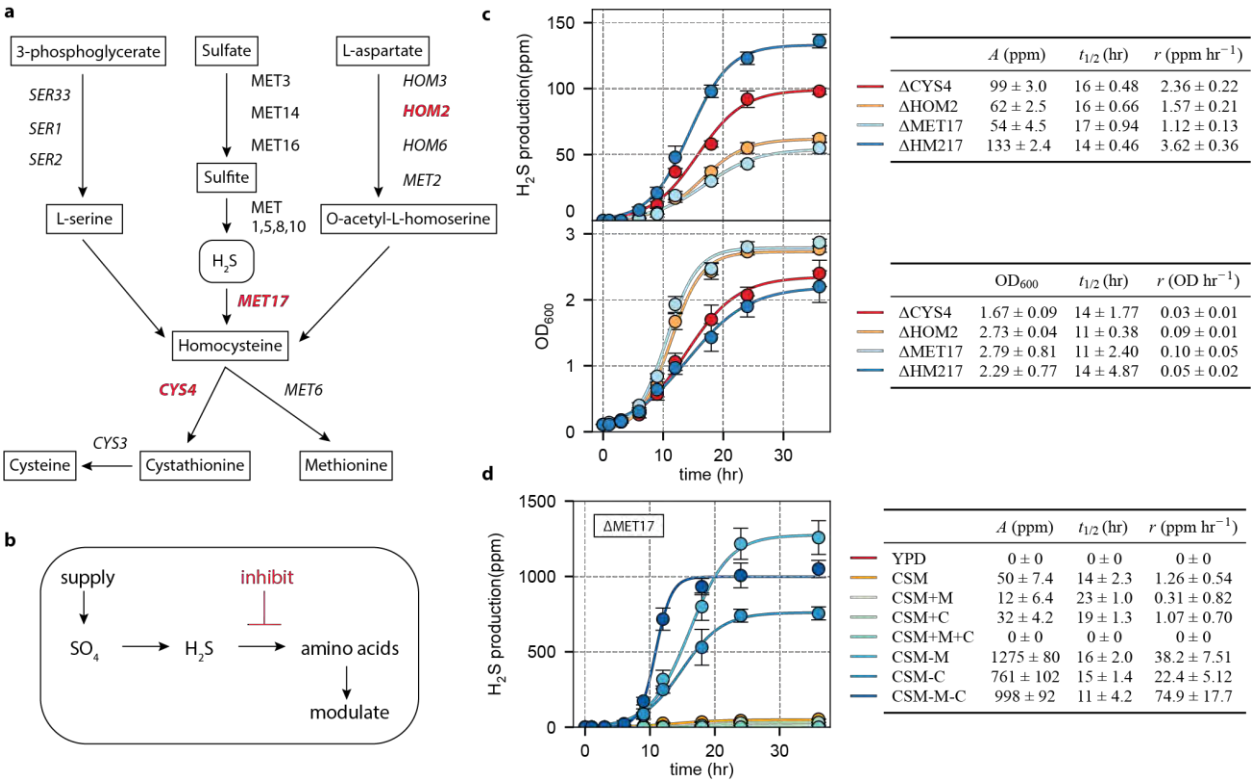

	A (ppm)	$t_{1/2}$ (hr)	r (ppm hr^{-1})
ΔCYS4	99 ± 3.0	16 ± 0.48	2.36 ± 0.22
ΔHOM2	62 ± 2.5	16 ± 0.66	1.57 ± 0.21
ΔMET17	54 ± 4.5	17 ± 0.94	1.12 ± 0.13
ΔHM217	133 ± 2.4	14 ± 0.46	3.62 ± 0.36

	OD_{600}	$t_{1/2}$ (hr)	r (OD hr^{-1})
ΔCYS4	1.67 ± 0.09	14 ± 1.77	0.03 ± 0.01
ΔHOM2	2.73 ± 0.04	11 ± 0.38	0.09 ± 0.01
ΔMET17	2.79 ± 0.81	11 ± 2.40	0.10 ± 0.05
ΔHM217	2.29 ± 0.77	14 ± 4.87	0.05 ± 0.02

	A (ppm)	$t_{1/2}$ (hr)	r (ppm hr^{-1})
YPD	0 ± 0	0 ± 0	0 ± 0
CSM	50 ± 7.4	14 ± 2.3	1.26 ± 0.54
CSM+M	12 ± 6.4	23 ± 1.0	0.31 ± 0.82
CSM+C	32 ± 4.2	19 ± 1.3	1.07 ± 0.70
CSM+M+C	0 ± 0	0 ± 0	0 ± 0
CSM-M	1275 ± 80	16 ± 2.0	38.2 ± 7.51
CSM-C	761 ± 102	15 ± 1.4	22.4 ± 5.12
CSM-M-C	998 ± 92	11 ± 4.2	74.9 ± 17.7

Figure 1 | Engineering the yeast sulfate assimilation pathway to generate H_2S. (**a**) Schematic adapted from Linderholm et. al.[30] Genes involved in the conversion of H_2S to amino acids were knocked out. Italicized knockouts were screened for H_2S production, while bolded red knockouts gave noticeable production of H_2S. (**b**) Deletant ΔCYS4, ΔHOM2, ΔMET17, and ΔHM217 produced sulfide which followed Le Chatelier's principle as supplying sulfate (reactants) while limiting nutrients such as cysteine and methionine (products) motivated the production of sulfide. (**c**) H_2S production (top curves) in relation to growth curves (bottom curves) in 50 mL CSM cultures. Fitted parameters A represents the steady-state production of H_2S, $t_{1/2}$ represents the time at which sulfide production reached half-max, and r the maximum rate of H_2S production. (**d**) H_2S production as a function of media composition for ΔMET17 with fitted

parameters A, $t_{1/2}$, and r. For all data, the mean $\pm$ s.d. of three replicates from different days are shown. Curves were fitted and parametrized against the sigmoid function $\frac{A}{1+e^{-k(t-t_0)}}$.

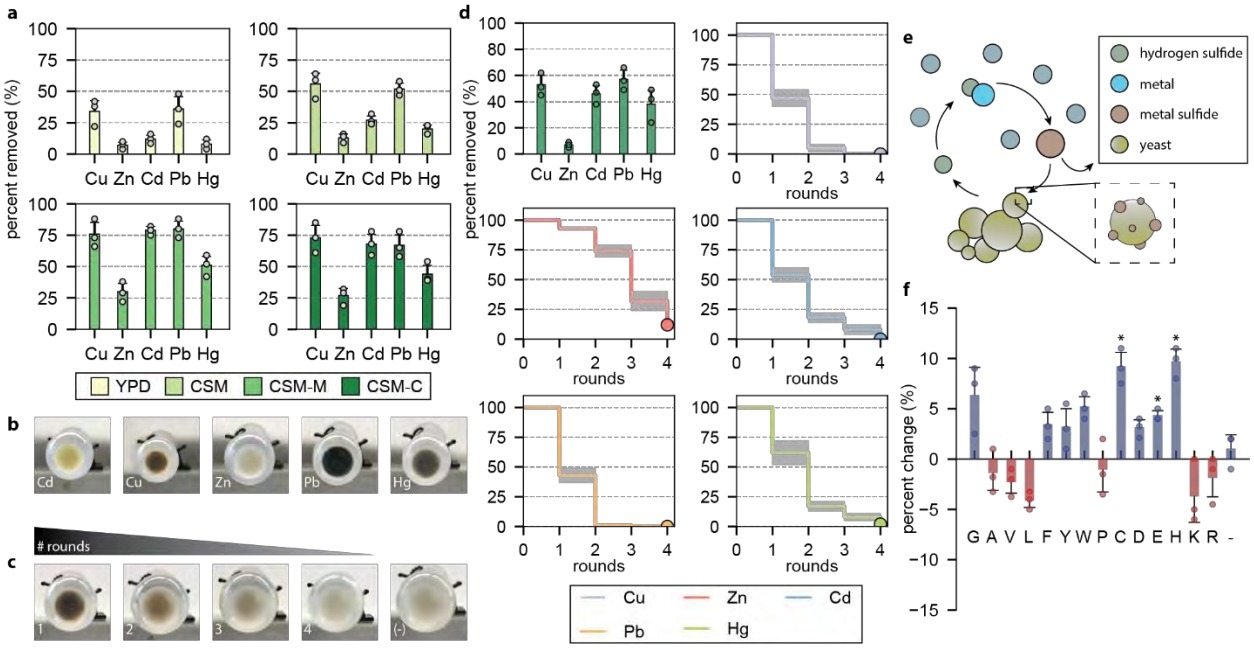

Figure 2 | Uptake of Cu, Zn, Cd, Pb and Hg with ΔMET17 sulfide-producing strains. (**a**) Bar chart represents percent precipitation of metals under varying culture conditions. –M and –C indicate media without methionine or cysteine, respectively. (**b**) Visual representation of metal sulfide precipitation in cultures incubated with 100 μM metals. (**c**) ΔMET17 with Cu, Zn, Cd, Pb and Hg all at 100 μM were cultured together for multiple rounds of precipitation. Images represent sequential removal of metals via precipitation, with the darker precipitated color gradually diminishing with increased number of rounds. (-) represents a yeast culture without any metals added. (**d**) Data representing images in (c). Top left plot represents the uptake from the first round. Remaining plots represent the gradual reduction of metal in solution after each round of precipitation. (**e**) Illustration of the hypothesized reaction of metal sulfides on the yeast surface. Metals could either precipitate in solution or on the yeast surface (**f**) Bar chart represents the percent change in cadmium precipitation given expression of hexa-peptide repeats of the amino acids designated on the x-axis. For all data, the mean $\pm$ s.d. of three replicates are shown.

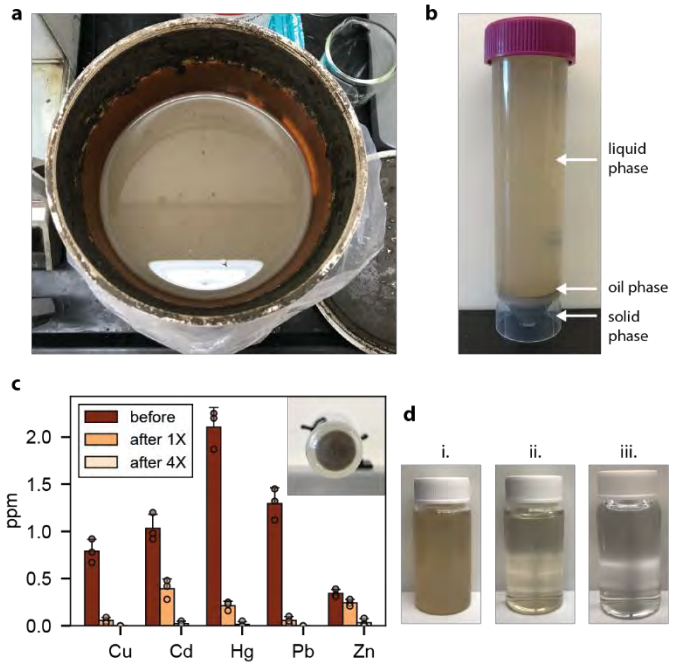

Figure 3 | Treatment of effluent from the Athabasca Oil Sands using sulfide-producing yeast. (**a**) Isolated effluent taken from the Athabasca Oil Sands. (**b**) Effluent was centrifuged to separate the liquid, oil, and solid phase, with the liquid phase used to test for yeast induced metal precipitation. (**c**) 1:1 mixture of liquid phase effluent to CSM-M culture with ΔMET17 incubated overnight and measured for metal content. After one round, the supernatant was transferred to a fresh culture of ΔMET17 and experiment repeated up to 4 times, with each iteration measured for metal content using ICP. Top right inlet image shows pelleted cell culture with precipitated waste after 1 round. (**d**) Visual inspection of wastewater opacity before (i) and after (ii) one round of yeast induced metal precipitation. (iii) Same sample after 4 rounds of yeast induced chemical precipitation. For all data, the mean ± s.d. of three replicates are shown.

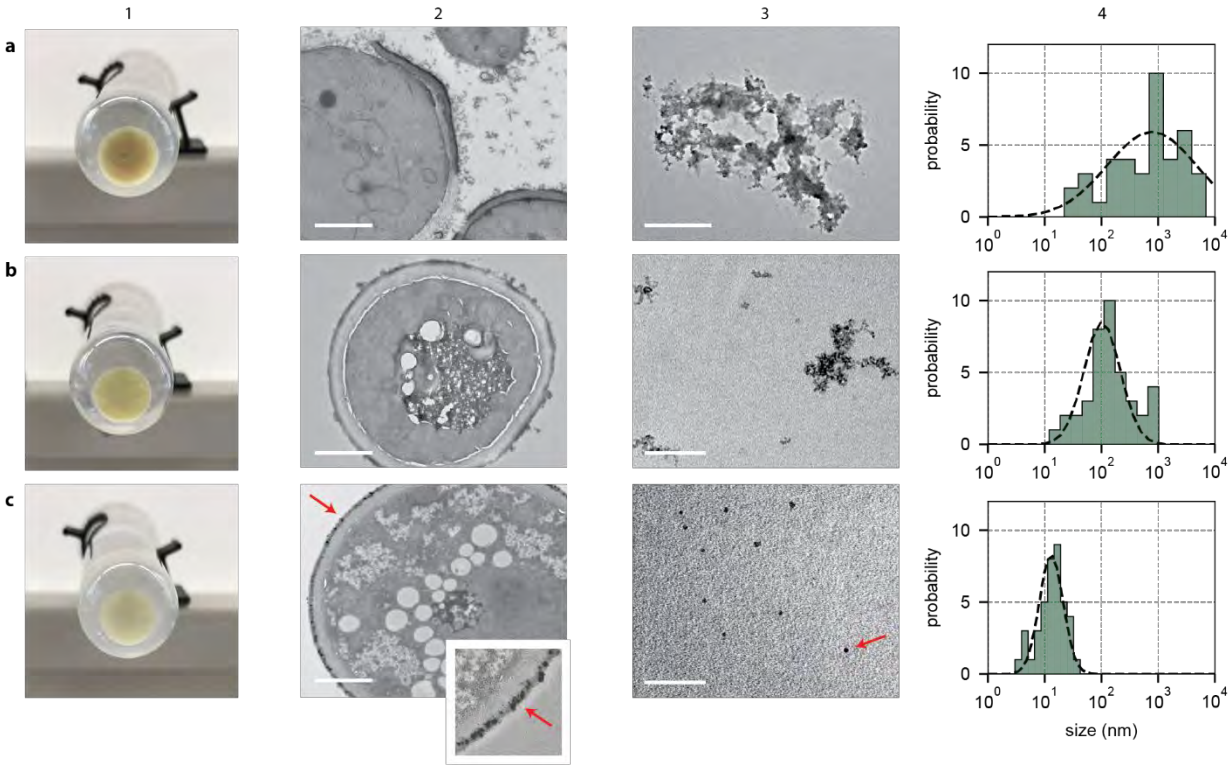

Figure 4 | Controlled size distribution of cadmium sulfide particles by controlling sulfide production rates. Columns are ordered as follows: image of metal precipitate (1), cell sectioned with metal precipitates (2), isolated metal precipitate (3), and counted size distribution of isolated metal precipitate (4). (**a**) ΔMET17 grown in CSM-M, (**b**) ΔMET17 grown in CSM-C, and (**c**) ΔMET17 grown in CSM. Column 2 scale bars are 1 μm. Column 3 scale bars are 1 μm for row A, and 100 nm for row B and C.

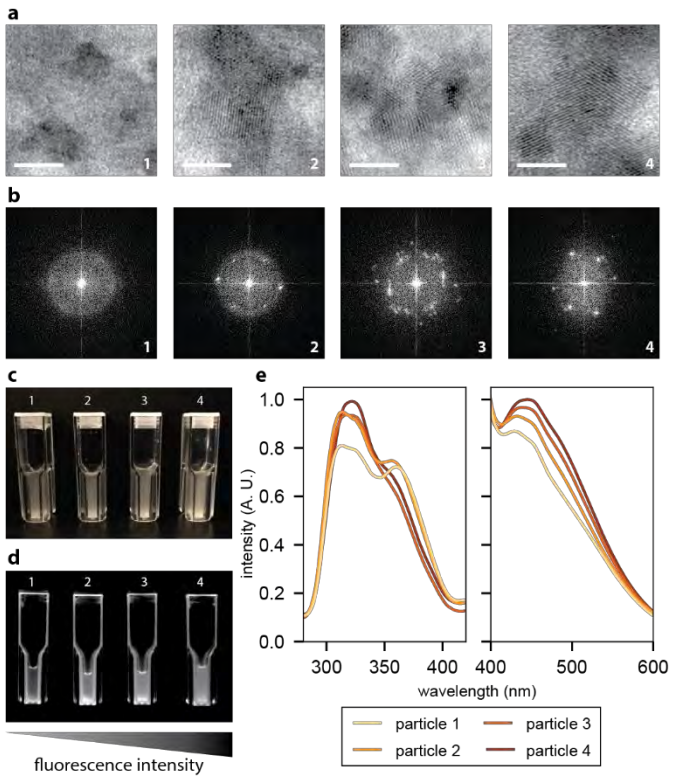

Figure 5 | Analysis of isolated precipitated cadmium sulfide particles as a function of hexa-amino acid displayed peptides. Particle numberings are: 1 = GGGGGG, 2 = CCCCCC, 3 = GGCGGC, 4 = GCCGCC. (**a**) Rows 1–4 show high resolution TEM images of precipitated cadmium sulfide particles displaying various degrees of lattice fringes. Scale bars represent 5 nm. (**b**) Fourier transform of cadmium sulfide particles showing various degrees of diffraction patterns caused by lattice fringes. (**c**) Image of isolated cadmium sulfide suspended in water of samples 1 through 4 in ambient light. (**d**) Same images captured under UV excitation. (**e**) Excitation and emission spectra of samples 1 through 4. Excitation peak converged towards 330 nm and emission peak towards 450 nm with increasing crystallinity.